ELSEVIER

Copepod diffusion within multifractal phytoplankton fields

C. Marguerit [a,*], D. Schertzer [a], F. Schmitt [b], S. Lovejoy [c]

[a] *Laboratoire de Modélisation Mécanique (L.M.M.), Université Pierre et Marie CURIE (Paris 6), C.N.R.S. - U.R.A. 229, Tour 66, 4, place Jussieu, 75252 Paris Cedex 05, France*
[b] *Section Climatologie Dynamique, Institut Royal Météorologique, Brussels, Belgium*
[c] *Physics Department, Mc Gill University, Montreal, Canada*

Abstract

Oceanic turbulence has been considered for a while as one of the main sources of the heterogeneity of the phytoplankton field over a wide range of scales. However, it is only recently that the intermittency of turbulence has been taken into account, although it is rather indispensable in the explanation of the observed patchiness of the plankton field. In order to improve the understanding and characterization of the diffusion of copepods within an heterogeneous phytoplankton field, we developed a model based on particle diffusion in a multifractal field. After discussing this model with some detail, we used it and the corresponding numerical simulations in order to investigate the fundamental question: does the strong heterogeneity of the phytoplankton generate a anomalous diffusion of the copepods? Although a positive answer is obtained in a rather straightforward manner for a one-dimensional multifractal field of phytoplankton concentration, the answer is rather more involved for a greater (topological) dimension of the field, contrary to some previous claims. © 1998 Elsevier Science B.V. All rights reserved.

Keywords: copepods; phytoplankton; turbulence; numerical simulations

1. Introduction

Understanding the effect of the oceanic turbulence on secondary production, i.e. the transfer of organic matter from phytoplankton to zooplankton, is a challenging objective. In particular, one would like to know how much the development of turbulence increases the predator–prey contact rate, favorising the zooplankton. The existence of intimate relationships between physical and biological processes has been previously considered (Denman and Powell, 1984; Legendre and Demers, 1984; Mackas et al., 1985),

due to the observed coupling between the distribution of phytoplankton populations and the structure of their physical environment over a wide range of spatial and temporal scales (Haury et al., 1978; Steele, 1985). However, in order to demonstrate it and understand it better, one needs to simulate the involved biological and physical processes on a similar range of scale. Unfortunately, this cannot be done by direct numerical simulations due at least to the rather limited memory size of our computers. The classical approach (Malchow and Shigesada, 1994) corresponds to truncating the original set of governing equations in a narrow band of scales (e.g. with a scale ratio of the order which is at best of one hundred on supercomputers), which is turn requires

* Corresponding author. Tel.: (+33-1) 014 427-3525/(4963); Fax: (+33-1) 014 427-5259; E-mail: margueri@lmm.jussieu.fr

ad hoc parametrizations (the so called sub-grid modelling). Instead, we consider a multifractal modelling of the fields, i.e. a stochastic modelling physically based on the scale symmetries of the original equations. These symmetries are immediately lost as soon as the corresponding equations are truncated. Space and/or time multifractal modelling has been originally developed for hydrodynamic turbulence, clouds and rain fields. More precisely, these techniques will be used in order to simulate the phytoplankton field advected by oceanic turbulence, as discussed in Section 2. The copepod diffusion —diffusion being understood in the sense of displacement of inert or living particles within a media (Okubo, 1980)— will be controlled by a local diffusivity depending on the local concentration of the phytoplankton (see Section 3). Corresponding to the notion of zooplankton grazing, the general rule to be followed is that this diffusivity should decrease with phytoplankton concentration, since copepods linger where the food is most abundant, and move away from where the food is scarce. Therefore, we have to study the diffusion of particles in a multifractal media. This diffusion is expected to behave quite differently from the classical and so called 'normal' diffusion in homogeneous media, which corresponds to Brownian particle walks (e.g. Gouyet, 1992). Indeed, this anomalous diffusion should reflect at a given level the intermittency of the medium, i.e. particle walks should have bursts of speedy diffusion which do not exist in the case of normal diffusion. We will discuss how to characterize this anomalous diffusion and we will show that one cannot rely on the classical method of estimating the scaling of the average distance travelled by particles as a function of time.

2. Multifractal phytoplankton fields

2.1. Oceanic turbulence, its intermittency and the heterogeneities of the phytoplankton field

Oceanic turbulence corresponds to a cascade of eddies from large scale (e.g. waves and tides) down to a small scale of dissipation, in a similar way to atmospheric turbulence (Richardson, 1922; Kolmogorov, 1941). At the level of a first approximation, phytoplankton biomass may be considered as passively advected by it and therefore one may expect a statistical behaviour close to that of the passive scalar (temperature, salinity,...). Passive scalar advection was first theoretically investigated (Obukhov, 1949; Corrsin, 1951) in the framework of homogenous turbulence (Kolmogorov, 1941; Obukhov, 1941), i.e. considering implicitly quasi-Gaussian statistics. The process is therefore rather well defined by its spectral properties, since they correspond to Fourier analysis of second order moments. The power spectrum of the variance of the scalar field should scale like the energy spectrum, i.e. having the well-known '−5/3' power law. This had been indeed empirically confirmed (Platt, 1972; Platt and Denman, 1975).

However, turbulence is far from being homogeneous: it is indeed strongly intermittent, with bursts of activity inside of bursts of activity... This 'patchiness' (Batchelor and Townsend, 1949) corresponds to the fact that the rate of energy transfer and the variance fluxes of passive scalars from large to small scales exhibit at all scales fluctuations far from being quasi-Gaussian (Kolmogorov, 1962; Obukhov, 1962). In contrast to the Gaussian case, the determination of the corresponding probability distribution requires the determination of moments of higher orders. With the assumption of scaling, this determination reduces (see below) the estimation of the corresponding exponents. However, the latter develop an a priori infinite hierarchy and they remain rather indeterminable, especially for the highest orders which correspond to the most extreme variability. A further and manageable reduction is obtained in the framework of universal multifractals (Schertzer and Lovejoy, 1987a, 1989). As discussed below, the infinite hierarchy is then characterized by only a few relevant exponents. Recent analyses showed that the observed phytoplankton biomass is in agreement with universal multifractal spatial distribution (Seuront et al., 1996a) and the estimates of the universal multifractal parameters will be used to simulate intermittent turbulent phytoplankton fields.

2.2. Multifractal models of the intermittency of turbulence

A first model, which takes into account the fact that the eddies fill less and less space and concentrates more and more the flux of energy, is the

'β-model' (Novikov and Stewart, 1964; Mandelbrot, 1974; Frisch et al., 1978). This model considers a 'dead or alive' alternative for an eddy breaking into sub-eddies: the latter are either dead or alive. Iterating this process corresponds to a 'black and white' picture of intermittency: the activity of turbulence is zero everywhere with the exception of a fractal set, the so-called fractal support of turbulence (Mandelbrot, 1974). The intermittency is fully characterized by the (unique) fractal dimension (D_s) of this (geometric) set, or equivalently by the parameter β, which corresponds at the same time to the rate of concentration of turbulence and the inverse of the probability of survival for an off-spring:

$$\begin{aligned} \Pr\left(\epsilon_\lambda \geq \beta^{-1}\right) &= \beta \qquad \beta = \lambda^{-c} \\ \Pr\left(\epsilon_\lambda = 0\right) &= 1 - \beta \qquad c = d - D_s \end{aligned} \qquad (1)$$

Pr denotes the probability of the singularity ϵ_λ of the multifractal field at the scale ratio λ. c is the codimension corresponding to D_s in a d-dimensional embedding space. Schertzer and Lovejoy (1983a, 1985) showed that the 'dead or alive' alternative is over-simplistic, since as soon as one considers a 'weak or strong' assumption (the 'α-model', see Fig. 1), the black and white picture of intermittency disappears for a coloured one: the level of activity ranges from extremely weak (say red) to extremely strong (say green) with all the possible intermediates yielded by the combination of mixtures of weak and strong along the cascade process. Instead of having a unique fractal support, we obtain an embedding of sparser and sparser fractal sets, for more and more active turbulence. This corresponds to the notion of multifractals (Parisi and Frisch, 1985). One may note that the p-model (Meneveau and Sreenivasan, 1987) corresponds to a micro-canonical version of the α-model, i.e. a conservation realization per realization instead of an ensemble conservation corresponding to canonical cascades (e.g., α-model).

Despite their pedagogic interest, these models have many drawbacks. One in particular drawback is
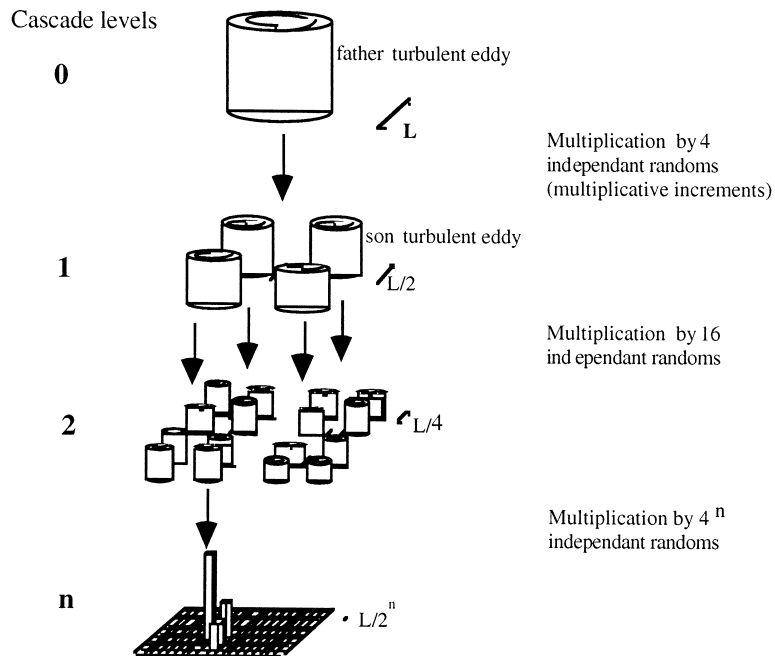

Fig. 1. Scheme of a (discrete) multiplicative cascade. This cascade is developed from the outer scale L (homogeneous eddy, i.e. its activity: $\epsilon_0(x) = 1$) to the scale $\ell_n = (L/\lambda_0^n)$ where n is the step of the cascade (cascade levels). $\lambda_0 = 2$ is the (discrete) scale ratio of the cascade, where the distribution of $\epsilon_n(x)$ is extremely inhomogeneous. Fractions of activity transmitted from parent eddies to each of their N ($= \lambda_0^d$) off-spring are identically independently distributed (i.i.d.) random variables, i.e. the activity level of a given off-spring is the product of that of its parents by this i.i.d. 'multiplicative increment' corresponding to this fraction. For simplicity sake, a two-dimensional cut of this cascade is presented. The eddies energy is proportional to their height.

that of being discrete in scale, i.e. the cascade proceeds by a fixed scale ratio ($\lambda_0 > 1$). Before seeing how to overcome these limitations by including continuous cascade models (Schertzer and Lovejoy, 1987a), we need to consider the statistical characterizations of multifractal fields.

2.3. Statistics of multifractal fields

The β-model and α-model are the simplest multiplicative (discrete) cascade models, which are obtained by considering that the fractions of activity (e.g., fractions of the flux of energy or scalar variance) transmitted from parent eddies to their offspring are identically independent distributed (i.i.d.) random variables. In other words the activity level of a given off-spring is the product of the activity level of its parent by this i.i.d. 'multiplicative increment' corresponding to this fraction. The non-trivial limit of the process down to infinitesimal small scale corresponds to infinite products of i.i.d. multiplicative increments. The independence of these increments leads to the following scaling behaviour (Schertzer and Lovejoy, 1987a) for the q-th order statistical moment of the field ϵ_λ at the scale ratio $\lambda = (L)/(\ell)$ where ℓ is the corresponding scale and L is the maximal scale of the process:

$$\left\langle \left(\epsilon_\lambda \right)^q \right\rangle \propto \lambda^{K(q)} \tag{2}$$

$K(q)$ is the scaling function of the moments, the prefactor being a constant or a slowly varying function of λ (e.g. $\log(\lambda)$). Since, under rather general conditions, the determination of the probability distribution and of the statistical moments of a random variable are equivalent, one may expect also some analogue scaling behaviour for the probability distribution (see Fig. 2 for illustration):

$$\Pr\left(\epsilon_\lambda \geq \lambda^\gamma \right) \propto \lambda^{-c(\gamma)} \tag{3}$$

where γ is the 'singularity' or more precisely speaking the 'order of singularity': when positive, γ is indeed the algebraic order of divergence of the field ϵ_λ with the (increasing) scale ratio λ. $c(\gamma)$ is the statistical 'codimension function' (Schertzer and Lovejoy, 1992) which describes the sparseness of the field intensities: when smaller than the dimension of
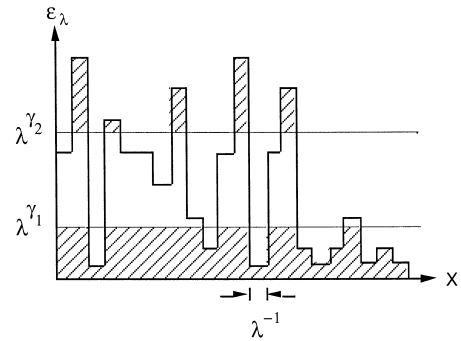

Fig. 2. The statistical codimension function $c(\gamma)$. A fundamental statistic of the cascade corresponds to measure the probability subspace where ϵ_λ (the field observed at a scale ratio $\lambda = (L/\ell)$ exceeds a (scaling) threshold λ^γ (γ being an arbitrary 'singularity'). This quantity should be scaling and its exponent $c(\gamma)$ is the statistical codimension function: $\Pr(\epsilon_\lambda > \lambda^\gamma) \approx \lambda^{-c(\gamma)}$. This figure shows clearly that corresponding to the fact that the strongest singularities are the rarest, $c(\gamma)$ is an increasing function, since the probability distribution decreases with $\gamma : \gamma_2 > \gamma_1 \Rightarrow c(\gamma_2) > c(\gamma_1)$.

the space in which the process is observed, the codimension is the difference between the dimension of space and the fractal dimension of the subset. This generalizes in many ways the (mono-) fractal relationship displayed in Eq. (1).

The relationship between moments and probability distribution implies a very simple relationship between the corresponding exponents: they are indeed related by the Legendre transform (Parisi and Frisch, 1985). This corresponds to:

$$K(q) + c(\gamma) = q \cdot \gamma \tag{4}$$

and a one-to-one relationship between orders of moments and of singularities:

$$\gamma = K'(q) \tag{5}$$

$$q = c'(\gamma) \tag{6}$$

It can be shown that $K(q)$ is convex, therefore $c(\gamma)$ is also convex since convexity is preserved by the Legendre transform. Furthermore, Eq. (3) implies that $c(\gamma)$ is positive and increasing (see Fig. 3 for illustration). These are the only mathematical constraints which should be satisfied by these two functions. At this level of generality, both functions depend on an infinite number of parameters. One may easily understand that they will be extremely
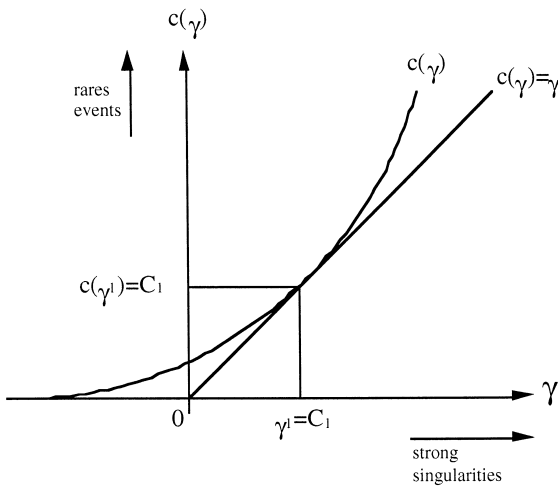
Fig. 3. Schematic representation of the $c(\gamma)$ function and its main properties. The $c(\gamma)$ function is positive, increasing and convex. For a conservative process, it is tangential to the bisectrice $c(\gamma) = \gamma$ at the point $C_1 = c(\gamma) = \gamma$ which measures the mean heterogeneity of multifractal fields.

difficult to empirically determine without any further assumption based on physical processes.

2.4. Universal multifractal fields

The general theme of routes to universality (Schertzer et al., 1991, 1995; Schertzer and Lovejoy, 1997) is that instead of considering only the iteration of the process down to smaller and smaller scales (Yaglom, 1966), one should first consider interactions of this process over a finite range of scales Λ with larger and larger numbers of its replicas, and then seek the limit when $\Lambda \to \infty$. This disproves the allegations of non-existence of any universality (Mandelbrot, 1989; Gupta and Waymire, 1993) based on some shortcomings of previous claims of universality.

A rather strong and straightforward universality corresponds to generators which are stable and attractive under addition (hence similar properties for fields under multiplication), via some more or less trivial renormalization (i.e. rescaling and/or recentring). In this case, generators and fields are defined by the following three universal exponents:

– H is the deviation from conservation of the mean fields: $H = 0$, the field is 'conservative', i.e.

strictly scale invariant on average; $H \neq 0$, the field is 'non-conservative';

– C_1 characterizes the mean heterogeneity of multifractal fields: it is the codimension of the mean field (see Fig. 4 for an illustration);

– α measures the multifractality of the field and is precisely defined as being the Lévy index of the generator: its values are bounded by $\alpha = 0$, corresponding to the (mono-) fractal 'β-model', and $\alpha = 2$, corresponding to the 'lognormal model' (Kolmogorov, 1962; Obukhov, 1962; Yaglom, 1966).

In the case of the phytoplankton biomass, we have the following estimates (Seuront et al., 1996a) for the time series: $H \approx 0.4$, $C_1 \approx 0.05$, $\alpha \approx 1.8$ (in space, 1 m–1 km, Tessier et al. (private communication, 1997) finds $H = 0.21 \pm 0.1$, $C_1 = 0.06 \pm 0.02$, $\alpha = 1.9 \pm 0.1$). One may note the following analytical expressions of the universal scaling functions $K(q)$ and $c(\gamma)$ (see Figs. 3, 5 and 6 for an illustration):

$$c(\gamma - H) = C_1 \cdot \left(\frac{\gamma}{C_1 \cdot \left(\frac{\alpha}{\alpha - 1} \right)} + \frac{1}{\alpha} \right)^{\frac{\alpha}{\alpha - 1}} \quad (7)$$

$$K(q) = \frac{C_1}{\alpha - 1} \cdot (q^\alpha - q) - q \cdot H \quad (8)$$

If, for any physical reason, the 'strong' universality fails to hold, weaker types of universality may still prevail (Schertzer et al., 1995) corresponding to different sub-classes of infinitely divisible generators (Novikov, 1994). For instance (as noted by She and Waymire, 1995), the log-Poisson statistics, considered by She and Leveque (1994) and Dubrulle (1994), provide a particularly simple example —which turns out to be a (non-renormalized) continuous limit of the α-model (Schertzer et al., 1995).

3. Simulation of the copepod diffusion

3.1. General considerations on diffusion

An animal diffusion in a (liquid) medium can be decomposed into a physical 'passive' diffusion and a biological 'active' diffusion (Okubo, 1980). The physical diffusion is due to the properties of fluid which surrounds the animal, the biological diffusion

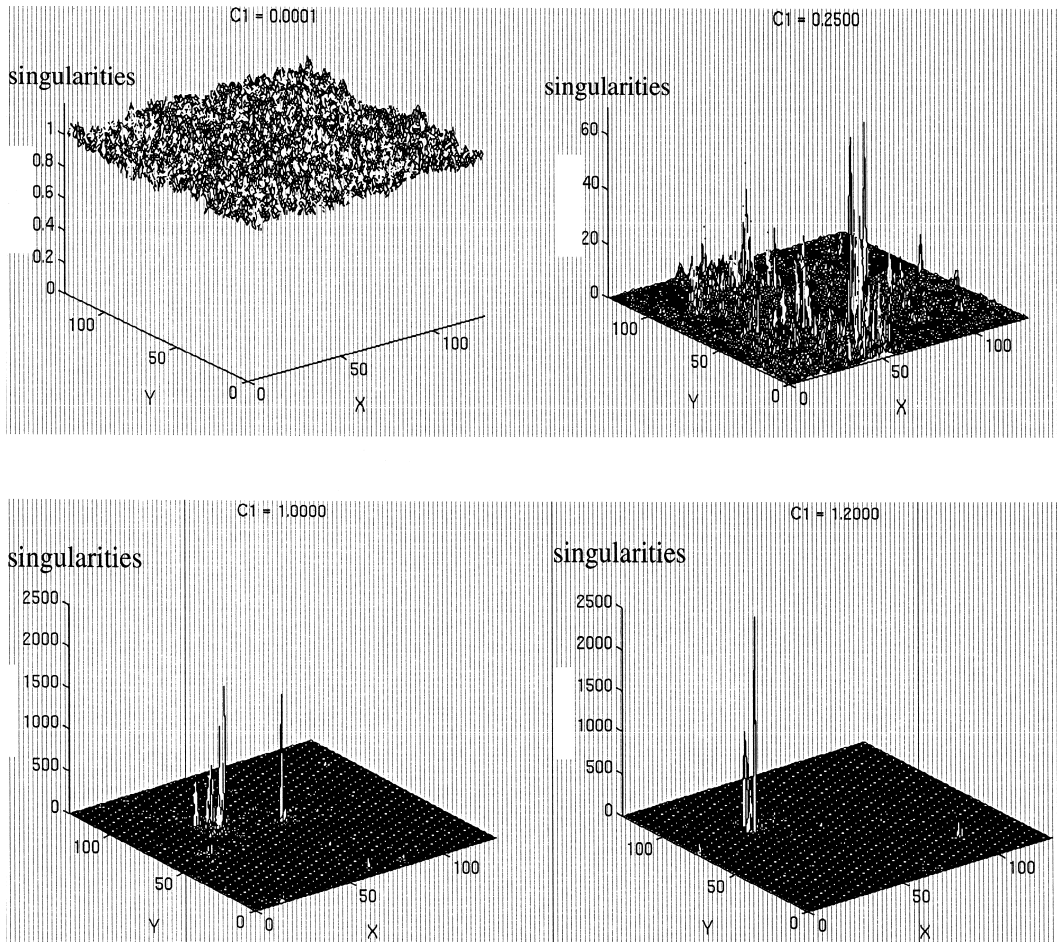Fig. 4. Variation of the mean heterogeneity of multifractal fields with C_1. From top right to bottom left, C_1 increases from 0.0001 to 1.2000 and correspondingly the (mean) inhomogeneity becomes higher and higher. In particular the higher singularity becomes larger and larger.
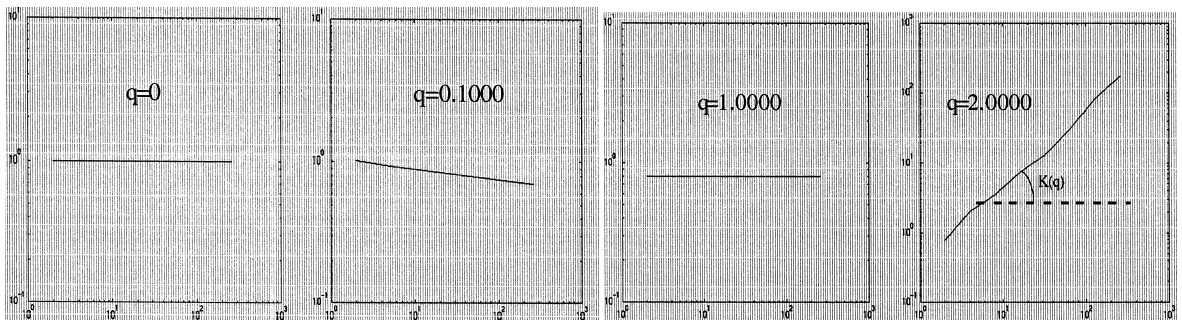

Fig. 5. Variation of the statistical moments in function of the scale ratio. Log–log plots statistical moments of order q vs. scale ratio (γ) of a numerically simulated conservative ($H = 0$) multifractal field (i.e. with a scale invariant mean). The estimate of the slope corresponds to an estimate of the scaling moment function $K(q)$. For $q = 0$, 1 $K(q) = 0$, corresponding respectively to conservation of the total probability and conservation of the mean. The change of signs ($K(0.1) < 0$, $K(2) > 0$) is due to convexity.
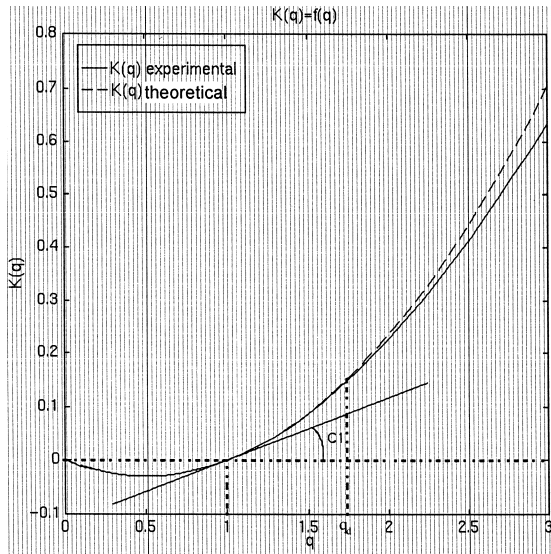
Fig. 6. Experimental and theoretical curves of the function $K(q)$ and its main properties. The function $K(q)$ is convex, positive and increasing for $q < 1$. Its tangent in $q = 1$ verifies $K'(1) = C_1 - H$ and $K(1) = -H$. In the conservative case, $H = 0$ and therefore $K'(1) = C_1$ and $K(1) = 0$. The observed divergence beyond a critical moment order q_s between the experimental and theoretical curves is due to the fact that the sample is finite (only one image of 1024×1024 pixels of the simulated field).

corresponds to the swim of the animal. Both can be cast into the rather general equation of diffusion:

$$\frac{\mathrm{d}p}{\mathrm{d}t} = \frac{\partial p}{\partial t} + \mathrm{div}(j) \tag{9}$$

where $p(x,t)$ is the probability density of finding a given number of particles at the location x and at time t, $(\mathrm{d})/(\mathrm{d}t)$ is the Lagrangian derivative (the global time differentiation following particles), $(\partial)/(\partial t)$ is the Eulerian derivative (the partial time differentiation at a fixed location), j is the flux (or current) of probability. The latter does correspond (by integration of Eq. (9)) to the number of particles exiting a given volume V (of finite surface ∂V):

$$\frac{\mathrm{d}}{\mathrm{d}t}P = \frac{\partial}{\partial t}P + J \tag{10}$$

$P(V,t)$ being indeed the probability of a given number of particles in the volume V at time t:

$$P(V,t) = \iiint_V p\,\mathrm{d}v \tag{11}$$

with the corresponding flux:

$$J = \iint_{\partial v} j \cdot \mathrm{d}s \tag{12}$$

Its conservation following any infinitesimal volume $\mathrm{d}v$ implies that the left hand side (l.h.s.) of Eq. (9) is zero, therefore:

$$\frac{\partial p}{\partial t} = -\mathrm{div}(j) \tag{13}$$

or for any elementary volume V (e.g., a pixel in numerical simulations)

$$\frac{\partial}{\partial t}P = J \tag{14}$$

These equations are often closed by assuming that the flux of the particle follows the gradient, i.e. by introducing a diffusivity coefficient κ:

$$j = -\kappa\,\mathrm{grad}(p) \tag{15}$$

when the diffusivity is homogeneous in space, one obtains the classical diffusion equation (the so-called Fick's diffusion):

$$\frac{\partial p}{\partial t} = \kappa \Delta p \tag{16}$$

which yields a Gaussian probability distribution for their location x (for particles initially released at time $t = 0$ from location $x_0 = 0$, with a zero velocity)

$$p(x,t) \propto \frac{1}{\sqrt{2\kappa t}} e^{-\frac{(x-x_0)^2}{2\kappa t}}$$

and the corresponding Langevin equation, i.e. kinematic equation of particles (at location x, with a characteristic friction time τ):

$$\frac{\mathrm{d}}{\mathrm{d}t}x(t) = \tau \cdot \gamma_0(t) \tag{18}$$

$$\langle \gamma_0(t)\gamma_0(t') \rangle = \frac{\kappa}{2}\delta(t-t') \tag{19}$$

γ_0 being a Gaussian white noise of correlation. However, since Richardson (1926) we know that Fickian diffusion does not hold true for turbulent flows at large Reynolds numbers, since indeed, we have:

$$J = uP - \kappa\,\mathrm{grad}(P) \tag{20}$$

and the first term (corresponding to advection by (turbulent) velocity field (u)) cannot be neglected at all and becomes of prime importance. At least, it introduces an effective scaling 'eddy diffusivity' κ_{ed} which is quite larger than the molecular diffusivity κ for scales above the (molecular) diffusive scale:

$$\kappa_{ed}^{(\ell)} \propto \epsilon^{\frac{1}{3}} \ell^{\frac{2}{3}} \tag{21}$$

3.2. Diffusion of plankton

We should consider at least two coupled equations of diffusion, one for the phytoplankton, the other one for the zooplankton. For both, the physical turbulent advection could be modelled with the help of a multifractal eddy diffusivity. On the other hand, the coupling could also be modelled for instance by introducing the Scheffer predator–prey model (Scheffer, 1991) into the hydrodynamic equations (Malchow and Shigesada, 1994). However, this paper aims to clarify some rather preliminary questions. Indeed, diffusion in a multifractal medium has been scarcely investigated. As discussed below, if the anomalous character of diffusion in a multifractal one-dimensional medium has been established (Havlin and Ben-Avraham, 1987; Silas et al., 1993, Lovejoy et al., 1996), and tackled with some theoretical arguments and corresponding numerical simulations, the situation seems somewhat unclear for two-dimensional and three-dimensional fields. We will, in particular, question the claims presented by Meakin (1987) that walks are anomalously slow for two-dimensional multifractal fields.

We therefore consider the simplest case of copepods diffusion in a frozen field of phytoplankton, i.e. we will neglect the feedback from the grazing to the concentration of the phytoplankton. In other words, we consider 'passive' walkers instead of 'active' walkers (e.g., Lam, 1995), the walk of the latter modifies the medium. On the other hand, turbulence signature will be only directly considered in the multifractal distribution of the phytoplankton, although the direct action of turbulence to the diffusion of zooplankton could be considered as being included in the definition of the diffusivity of the zooplankton generated by the phytoplankton. How-

ever, we will not discuss this issue in the present paper.

Finally, the diffusivity of the zooplankton generated by the phytoplankton will be defined by rather simple considerations: due to grazing activity, copepods should diffuse slower and slower as the phytoplankton concentration is higher and higher. So, this corresponds to taking diffusivity equal to negative powers of phytoplankton concentration. More generally, fractional integrations of negative powers of phytoplankton concentration could be considered. For the sake of simplicity, as well as for a comparison with one-dimensional results (Lovejoy et al., 1996), we will consider the inverse of a multifractal field considered as describing the phytoplankton concentration ρ:

$$\kappa = \frac{1}{\rho} \tag{22}$$

3.3. Discretization: the master equation

As soon as the diffusivity is non-homogeneous, there is no longer a known analytical solution (in contrast to Eq. (16)). However, one can proceed numerical simulations on a regular lattice (in our case a two-dimensional one), by considering the evolution of the probability of finding particles on a given pixel (see Fig. 7 for an illustration), i.e. of the probability density integrated over this pixel (Eqs. (14) and (15)). The corresponding master equation is the following (for the site o surrounded by N pixels i, $N = 4$ for $d = 2$)):

$$\frac{\partial}{\partial t} P_{i,t} = -\sum_{i=1}^{N} \bar{\kappa}_{o,i} (P_{i,t} - P_{o,t}) \tag{23}$$

where $\bar{\kappa}_{o,i}$ is the mean diffusivity at the interface of the two sites o and i which can be estimated by:

$$\bar{\kappa}_{o,i} = \frac{\kappa_o + \kappa_i}{2} \tag{24}$$

In order to obtain a finite time difference equation it is interesting to choose Δt, the time lag, as being the average local diffusivity time, i.e.:

$$\frac{\Delta t}{\eta^2} \frac{1}{\sum\limits_{i=1}^{N} \bar{\kappa}_{o,i}} \tag{25}$$
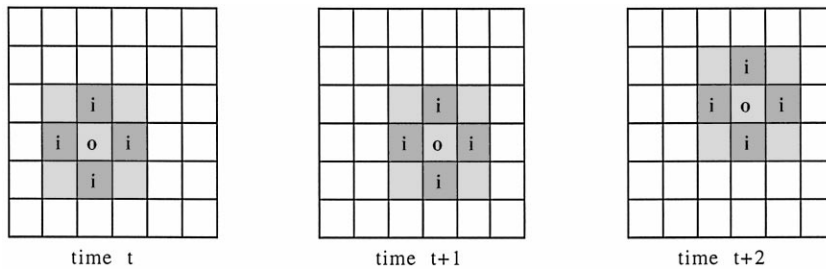
Fig. 7. The diffusion model. These schemes shows the pixels i where the copepod can go, starting from the pixel o in function of time t, $t + 1$, $t + 2$.

(η is the mesh size) which yields the following discretized equation:

$$P_{o,t+\Delta t} - P_{o,t} = - \sum_{i=1}^{N} (P_{i \to o,t} - P_{o \to i,t}) \qquad (26)$$

$P_{o \to i}$ is the probability that the copepod moves from o towards i such as:

$$P_{o \to i} = T_{o \to i} \cdot P_{(o,t)} \qquad (27)$$

and $T_{o \to i}$ is the 'normalized' transition rate from o towards i (probability during diffusivity time):

$$T_{o \to i} = T_{i \to o} = \frac{\overline{\kappa}_{o,i}}{\sum_{i=1}^{N} \overline{\kappa}_{o,i}} \qquad (28)$$

It is important to note that in this framework, the physical time is not proportional to the number of steps, but corresponds to the sum of the local times (Eq. (25)). The probability of finding a particle at location (x) at time t will be estimated by an ensemble of the average of series of a unique particle walk $X(t)$, i.e.:

$$p(x,t) = p(X(t) = x) = \langle \delta(X(t) - x) \rangle \qquad (29)$$

and conversely the indicator of the particle location $\langle \delta(X(t) - x) \rangle$ is ruled by the discrete master equation (Eq. (26)) with $P_{o,t} = 1$ (and $P_{i,t} = 0$) and its probability $P_{o \to i,t}$ to move from the site o to the site i is therefore merely given by the transition rate $T_{o \to i}$ (Eq. (28)). This corresponds to defining the arrival site according to the outcome of a random variable having N possible outcomes, their respective probability being given by the normalized transition rate.

3.4. Characterization of the particle diffusion

A standard way of characterizing particle diffusion corresponds to estimating the so called fractal dimension of their walks (d_w). It measures the (average) space occupation degree by their walks. It is the (mass) scaling exponent of the root mean square (r.m.s.) distance $\langle R^2 \rangle$ travelled by particles in time:

$$\langle R^2 \rangle^{\frac{d_w}{2}} \propto t \qquad (30)$$

If these walks are straight lines $d_w = 1$, whereas for the Brownian motion $d_w = 2$ which corresponds to the fact that Brownian walks are dense in the plane (e.g., Gouyet, 1992), i.e. to each double point there corresponds a non-visited site (see Figs. 8–10). If $d_w < 2$, the diffusion is anomalously fast and corresponds to a 'super-diffusivity'. Conversely, for $d_w > 2$, the diffusion is anomalously slow and corresponds to a 'sub-diffusivity'.

It is important to consider the limitation as well as the interest of this critical exponent for multifractal (and fractal) diffusivity. Indeed, in this case, it can be expected that the characterization of the walk will require an (infinite) hierarchy of exponents rather than a unique one. Nevertheless, it is already important to estimate this behaviour of the r.m.s. walk. Furthermore, some theoretical results, which are obtained from multifractal diffusivities on uni-dimensional space (Havlin and Ben-Avraham, 1987; Silas et al., 1993; Lovejoy et al., 1996) need to be tested on higher dimensions.

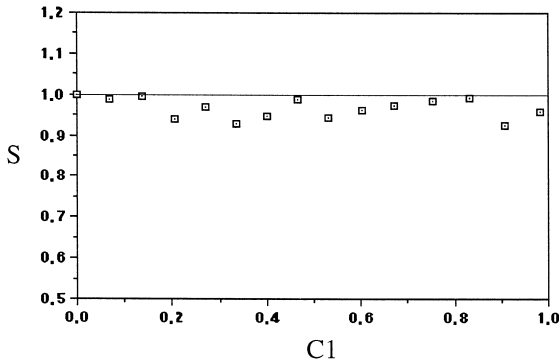Indeed, it has first been shown (Machta, 1981; Zwanzig, 1982) that in the case of (local) i.i.d.

Fig. 8. Near constancy of the diffusion exponent S and corresponding fractal dimension of the walk d_w. The two-dimensional multifractal plankton fields were simulated on 1024×1024 pixels and correspond to conservative universal multifractal fields having been Gaussian generated ($H = 0$, $\alpha = 2$, lognormal). Considering 15 values of C_1 regularly distributed between 0 and 1. For each value of C_1, 100 plankton fields were simulated, and for each plankton field 350 particle (copepod) diffusions were simulated yielding reasonable estimates of the scaling exponent $S = (2/d_w)$ fractal dimension of the walks S is not significantly different to 1 and does not display obvious trends related to increasing C_1: S oscillates between $S_{min} = 0.9231$ and $S_{max} = 1.0000$ with $S_{mean} = 0.9664$.

diffusivities on a uni-dimensional space, the effective diffusivity of a walk is merely the harmonic mean of the diffusivities of the N distinct visited sites.

$$\kappa_{eff}^{-1} \propto \frac{1}{N} \sum_{i=1}^{N} \kappa_i^{-1} \qquad (31)$$

Considering the diffusivity as the inverse of the phytoplankton concentration (Eq. (22)), it merely states that the concentrations of the visited sites summed up to yield the effective phytoplankton concentration ρ_{eff}.

The implications of Eq. (31) have been considered (Weissman and Havlin, 1988) for uni-dimensional multifractal fields. More recently Silas (1994), and Lovejoy et al. (1996) inferred from

$$\langle \kappa_{eff,\lambda} \rangle \propto \langle (\Sigma \rho_{i,\lambda})^{-1} \rangle \propto \lambda^{K(-1)} \qquad (32)$$

that:

$$d_w = 2 + K(-1) \qquad (33)$$

$K(-1)$ being positive (due to convexity of $K(q)$ and $K(0) = K(1) = 0$), Eq. (33) confirms that the walk is anomalously slow (as first noticed by Meakin (1987) on bi-dimensional multifractal fields) due to

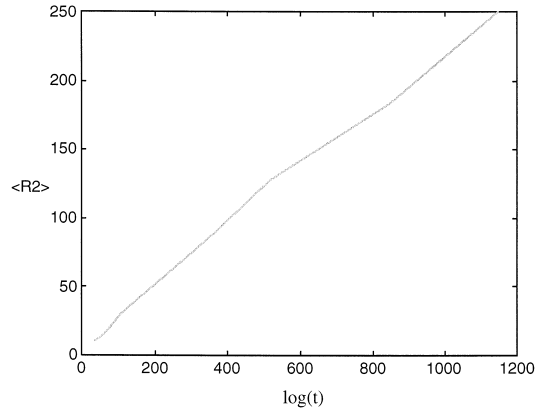Fig. 9. Curve $\log(\langle R^2 \rangle) = f(\log(t))$. This curve corresponds to a simulation of copepod diffusion in two-dimensional conservative multifractal phytoplankton fields. It shows the evolution of the distance travelled by the copepod as a function of time. The slope of this curve is the diffusion exponent $S \approx 1$.

the fact that particles are trapped in a hierarchy of barriers. Although this phenomenology is very appealing and rather clear in dimension one (Lovejoy et al., 1996), its generalization is not so straightforward for a dimension higher than one, for the simple reason that particles can then wind around these barriers, therefore the trapping is less and less effec-
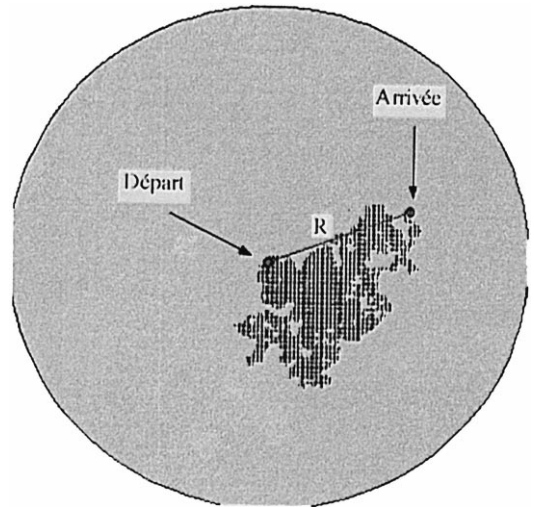

Fig. 10. Visualization of the different sites visited by the copepod in an homogeneous field. This figure, corresponding to a numerical simulation, shows clearly that in an homogeneous two-dimensional field, the Brownian walk of the copepod is dense in the plane. In this case, $d_w = 2$ and then $\langle R^2 \rangle \propto t$.

tive as the topological of the medium is increasing. In particular, we will discuss the claim of Meakin (1987) that diffusion in bi-dimensional multifractal fields is anomalous.

On the other hand, for uni-dimensional conservative universal multifractal concentration field having been Gaussian generated ($\alpha = 2$); the deviation of the fractal dimension of the walks from the normality ($d_w = 2$) is proportional to the mean heterogeneity of the latter (C_1), since due to Eqs. (8) and (33) we obtain:

$$d_w - 2 = 2C_1 \tag{34}$$

3.5. Numerical simulations of particle diffusion on a two-dimensional multifractal field

First, we have checked the diffusion results found in one dimension by Lovejoy et al. (1996) and we have verified for small multifractal lognormal fields about 1×512 pixels and for C_1 between 0.03 and 0.55 that effectively

$$S = \frac{2}{d_w} = \frac{2}{2 + 2C_1} = \frac{1}{1 + C_1} \tag{35}$$

Where S is the diffusion exponent.

For each value of C_1, 10 phytoplankton fields were simulated, and for each latter realization, 10 particle (copepod) diffusions were simulated.

Then, in order to investigate the question of particle diffusion on two-dimensional multifractal fields, we performed numerical simulation on work stations (H.P. 9000-700 and IBM SP2 390). The two-dimensional universal multifractal phytoplankton fields were simulated on 1024×1024 pixels; on the one hand, conservative fields having been Gaussian generated ($H = 0$, $\alpha = 2$, 'lognormal') (Fig. 9) for systematic comparison with the uni-dimensional results (Lovejoy et al., 1996); on the other hand non-conservative fields having been Levy generated ($H = 0.41$, $\alpha = 1.8$ ('Log-Levy')) in order to be closer to the observed multifractality of the phytoplankton fields (Seuront et al., 1996a).

With simulations of the conservative universal multifractal fields having been Gaussian generated ($H = 0$, $\alpha = 2$), we tested systematically the possible dependence of the fractal dimension of the walk on the mean heterogeneity of the plankton field (as is the case in the unidimensional case, Eq. (34)), considering 15 values of C_1 regularly distributed between 0 and 1. For each value of C_1, 100 plankton fields were simulated, and for each of these fields 350 particle (copepod) diffusions were simulated. The last figure was empirically observed as a yielding, rather than a straight line for the curve $\log(\langle R^2 \rangle) = f(\log(t))$ (see Fig. 9), i.e. reasonable estimates of the scaling exponent $S = (2)/(d_w)$, where d_w is the fractal dimension of the walks. We obtain estimates of d_w which oscillate between 2.17 and 2.00 (i.e., $0.92 < 1.00$), without any (increasing) trend with C_1 (see Fig. 8). We have similar results for the series of diffusions on non-conservative fields having been Levy generated, although we have not been as systematic in exploring the mean heterogeneity values (C_1). It is important to note that in this case $K(-1) = \infty$; which requires the consideration of the associate multifractal phase transition (Schertzer and Lovejoy, 1992) in order to be fully understood.

On the other hand, the visualizations of copepod walks (see Fig. 11 and Fig. 12) show clearly that they are far from being as homogeneous as a Brownian motion: copepods do stay longer in the (scarce) regions of high phytoplanktonic concentrations, therefore having a rather convoluted walk, although not getting fully trapped, whereas in the (wide) low phytoplankton concentration areas, they have more linear trajectories.

Overall, it seems that the heterogeneity of the phytoplankton concentration field has little influence on the 'mean' scaling (more exactly the r.m.s. scaling) of the diffusion in dimension two. However, it seems to induce an heterogeneity of the walk which should be observable with the help of quantities related to other statistical moments of the walk, e.g.:

$$R^q(t) = \langle (\Sigma r_i^q) \rangle^{\frac{1}{q}} \tag{36}$$

where r_i are the elementary steps of the walk. This relation could be scaling with a full hierarchy of fractal dimensions. One may note that these quantities are rather different from $\langle (\Sigma r_i^2)^{\frac{q}{2}} \rangle^{\frac{1}{q}}$ considered by Meakin (1987) and which turn out to be
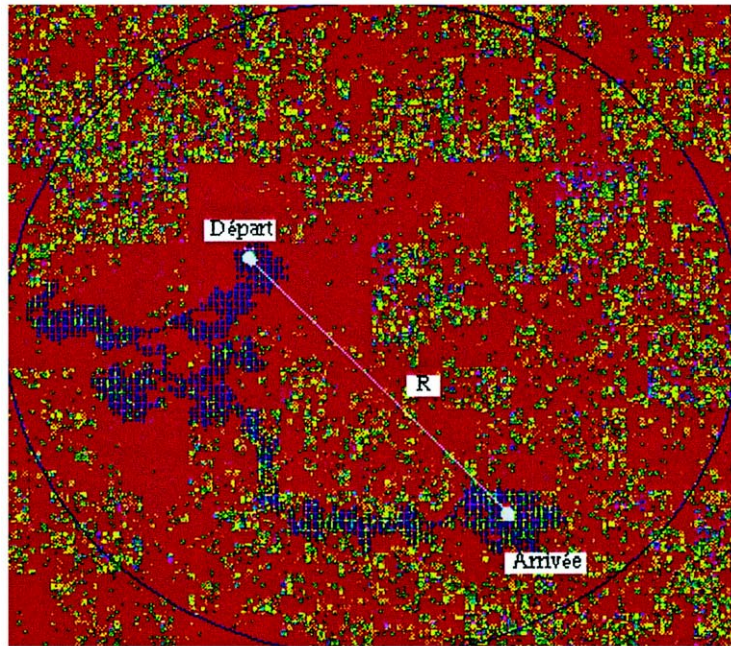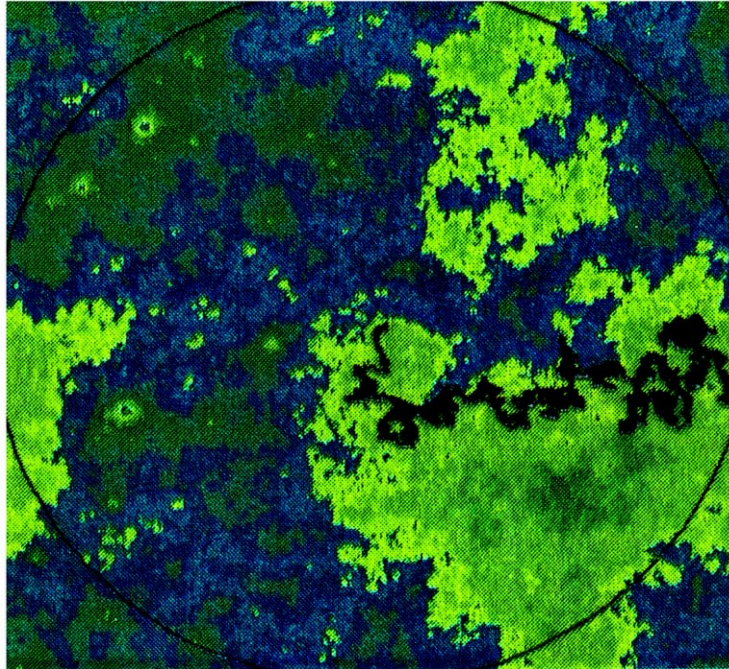
Fig.11

Fig.12

monoscaled, at least in the one dimensional case (Lovejoy et al., 1996).

$$R^q(t) \propto t^{\frac{1}{d_w}} \qquad (37)$$

This issue is developed elsewhere. Now it is important to compare our two-dimensional results with the ones reported by Meakin. As mentioned earlier, Meakin (1987) reported anomalous slow diffusion with two-dimensional multifractal fields (rather similar to the p-model). However, the scaling exponents are based on the number of steps rather than the physical time, both being rather different in the case of strongly inhomogeneous fields. We obtain larger estimates of d_w when using the number of steps instead of the physical time.

4. Conclusions and perspectives

We argued that the understanding and modelling of the diffusion of copepods in highly inhomogeneous phytoplankton concentrations and physical properties of the ocean require a preliminary clarification on the diffusion of particles in a multifractal medium.

We showed that the general phenomenology of the latter corresponds to particles being often trapped by hierarchies of higher and higher phytoplankton concentrations, therefore we expect that the diffusion is anomalously slow or 'sub-diffusive', in comparison to the normal diffusion.

For a one-dimensional medium, we checked that the 'mean' scaling (more exactly the r.m.s. scaling) of the walk corresponds indeed to sub-diffusivity, and more precisely to the theoretical and numerical results obtained by Silas et al. (1993) and Lovejoy et al. (1996).

However, we pointed out that the topological dimension one is very special, since it prevents the particles from winding around the barriers. Indeed, we presented a series of simulations on two-dimensional media which yield non-anomalous r.m.s. scaling exponents contrary to a previous claim (Meakin, 1987). We clarified that this claim was based on an exponent related to the number of steps, which is no longer proportional to the physical time of the walk in a highly inhomogeneous medium.

Therefore, the phenomenology of the diffusion is more subtle in a higher dimension than in dimension one: it is no longer measurable by standard considerations, because the particles are never fully trapped by high concentration spots, but rather wind around them. This requires therefore, to go beyond a fractal analysis with the help of a unique fractal dimension of the walk: the characterization of the inhomogeneity of the walk rather requires a multifractal analysis, i.e. the determination of a full hierarchy of fractal dimensions.

Although it would be interesting to check numerically that diffusion in three-dimensional multifractal fields behave the same as in two-dimensional fields, we faced some numerical limitations: with multifractal fields no larger than 128^3, we cannot obtain asymptotical results.

In future, we will take into account the feedback of the grazing on the concentration of phytoplankton and then on the copepod diffusion. Later on, we will test the direct action of turbulence on diffusion in

Fig. 11. Visualization of the different sites visited by the copepod during its grazing in a discrete lognormal multifractal phytoplankton field. Red, yellow and green areas correspond to higher and higher phytoplankton concentrations, whereas sites visited by the copepod are coloured in blue. The copepod is set free in a region of low phytoplankton concentrations (departure). Copepod walks are clearly far from being as homogeneous as a Brownian motion: copepods do stay longer in the regions of high phytoplankton concentrations where they have a rather convoluted walk, although not getting fully trapped, whereas in the (wide) low plankton concentration areas, they have more linear trajectories.

Fig. 12. Visualization of the different sites visited by the copepod during its grazing in a continuous log-Lévy multifractal phytoplankton field. Blue, yellow and green areas correspond to higher and higher phytoplankton concentrations, whereas sites visited by the copepod are coloured in black. The copepod is set free in an boundary layer between regions of low and high phytoplankton concentrations (centre of the field). As in the lognormal multifractal phytoplankton field (Fig. 11), copepod walks are clearly far from being as homogeneous as a Brownian motion: copepods do stay longer in the regions of high phytoplankton concentrations where they have a rather convoluted walk, although not getting fully trapped, whereas in the (wide) low plankton concentration areas they have more linear trajectories.

simulating real non-frozen turbulent multifractal fields.

Another direction of further investigations corresponds to consider generalized diffusion equations (Chechkin et al., 1995) in multifractal media. These equations are obtained by replacing standard differential operators by fractional integrations. They already yield anomalous diffusion in homogeneous media, since the corresponding walks are no longer Gaussian, but Levy stable. Furthermore, these equations can be used to obtain the generators of the universal (space–time) cascades (Marsan et al., 1996; Schertzer et al., 1997). It would be therefore not justified to only analyse the effect of the inhomogeneities of the latter to a diffusion ruled by the normal diffusion equation, when these inhomogeneities are more directly related to the generalized diffusion equations.

A general consequence of this paper for ecology is that the classical way of estimating the primary and secondary productions of the biomass only on a large scale seem rather untenable. On the contrary, not only do we need to understand the predator–prey system on a wide range of scale, but this could be achieved in the framework of multifractals. We have highlighted the main theoretical steps to be further undertaken, however they also suggest corresponding developments of empirical experiments.

Acknowledgements

References

Batchelor, G.K., Townsend, A.A., 1949. The nature of turbulent motion of large wavenumbers. Proc. Roy. Soc. A 0000, 199–238.

Chechkin, A.V., Schertzer, D., Tur, A.V., Yanovsky, V.V., 1995. Generalized Fokker–Planck equation for anomalous diffusion. Ukr. J. Phys. 40 (5), 434–439.

Corrsin, S., 1951. On the spectrum of isotropic temperature in an isotropic turbulence. J. Appl. Phys. 22, 469–473.

Denman, K.L., Powell, T.M., 1984. Effects of physical processes on planktonic ecosystems in the coastal ocean. Oceanogr. Mar. Biol. Ann. Rev. 22, 125–168.

Dubrulle, B., 1994. Intermittency in fully developed turbulence: log-poisson statistics and generalized scale covariance. Phys. Rev. Lett. 73 (7), 959–962.

Frisch, U., Sulem, P.L., Nelkin, M., 1978. A simple dynamical model of intermittent fully developed turbulence. J. Fluid Mech. 87, 719.

Gouyet, J.F., 1992. Physique et structures fractales. Masson, Paris, 46.

Gupta, V.K., Waymire, E.C., 1993. A statistical analysis of mesoscale rainfall as a random cascade. J. Appl. Meteor. 32, 251–267.

Haury, L.R., McGowan, J.A., Wiebe, P.H., 1978. Patterns and processes in the time–space scales of plankton distributions. In: Steele, J.H. (Ed.), Spatial Pattern in Plankton Communities. Plenum, New York, pp. 277–327.

Havlin, S., Ben-Avraham, D., 1987. Diffusion in disordered media. Adv. Phys. 36 (6), 695–798.

Kolmogorov, A.N., 1941. Local structure of turbulence in an incompressible liquid for very large Reynolds numbers. Proc. Acad. Sci. USSR, Geochem. Sect. 30, 299–303.

Kolmogorov, A.N., 1962. A refinement of previous hypotheses concerning the local structure of turbulence in a viscous incompressible fluid at high Reynolds number. J. Fluid Mech. 13, 82.

Lam, L., 1995. Active walker models for complex systems. Chaos Solitons Fractals 6, 267–285.

Legendre, L., Demers, S., 1984. Towards dynamic biological oceanography and limnology. Can. J. Fish. Aquat. Sci. 41, 2–19.

Lovejoy, S., Schertzer, D., Silas, P., 1996. Diffusion in one dimensional multifractals. Submittted to Phys. A.

Machta, J., 1981. Generalized diffusion coefficient in one-dimensional random walks with static disorder. Phys. Rev. B 24, 5260–5269.

Mackas, D.L., Denman, K.L., Abbot, M.R., 1985. Plankton patchiness: biology in the physical vernacular. Bull. Mar. Sci. 37, 652–674.

Malchow, H., Shigesada, N., 1994. Nonequilibrium plankton community structures in an ecohydrodynamic model system. Nonlinear Proc. Geophys. 1, 3–11.

Mandelbrot, B., 1974. Intermittent turbulence in self-similar cascades: divergence of high moments and dimension of the carrier. J. Fluid Mech. 62, 331–350.

Mandelbrot, B., 1989. Fractal geometry: what is it and what does it do? In: Fleischman, M., Tildesley, D.J., Ball, R.C. (Eds.), Fractals in the Natural Sciences. Princeton University Press, Princeton, pp. 3–16.

Marsan, D., Schertzer, D., Lovejoy, S., 1996. Causal space–time multifractal modelling of rain. J. Geophys. Res. 31D, 26333–26346.

Meakin, P., 1987. Random walks on multifractal lattices. J. Phys. A 20, L771–777.

Meneveau, C., Sreenivasan, K.R., 1987. Simple multifractal cascade model for fully develop turbulence. Phys. Rev. Lett. 59 (13), 1424–1427.

Novikov, E.A., Stewart, R., 1964. Intermittency of turbulence and spectrum of fluctuations in energy-dissipation. Izv. Akad. Nauk. SSSR. Ser. Geofiz. 3, 408–412.

Novikov, E.A., 1994. Infinitely divisible distributions in turbulence. Phys. Rev. E 50 (5), R3303–3305.

Obukhov, A.M., 1941. Spectral energy distribution in a turbulent flow. Dokl. Akad. Nauk SSSR 32 (1), 22–24.

Obukhov, A.M., 1949. Structure of the temperature field in a turbulent flow. Izv. Akad. Nauk. U.S.S.R. Geogra. I Geopfiz. 13, 55–69.

Obukhov, A.M., 1962. Some specific features of atmospheric turbulence. J. Fluid Mech. 13, 77.

Okubo, A., 1980. Diffusion and Ecological Problems: Mathematical Models. Springer, Berlin.

Parisi, G., Frisch, U., 1985. A multifractal model of intermittency. In: Ghil, M., Benzi, R., Parisi, G. (Eds.), Turbulence and Predictability in Geophysical Fluid Dynamics and Climate Dynamics. North-Holland, Amsterdam, p. 84.

Platt, T., 1972. Local phytoplankton abundance and turbulence. Deep-Sea Res. 19, 183–187.

Platt, T., Denman, K.L., 1975. Spectral analysis in ecology. Annu. Rev. Ecol. Syst. 6, 189–210.

Richardson, L.F., 1922. Weather prediction by numerical process. Cambridge University Press, republished by Dover, 1965.

Richardson, L.F., 1926. Atmospheric diffusion shown on a distance–neighbour graph. Proc. R. Soc. A 110 (756), 709–737.

Scheffer, M., 1991. Fish and nutrients interplay determines algal biomass: a minimal model. Oikos 62, 271–282.

Schertzer, D., Lovejoy, S., 1983. Symposium on turbulence and chaotic phenomena in fluids. U.I.T.A.M., Preprint, pp. 141–144.

Schertzer, D., Lovejoy, S., 1985. The dimension and intermittency of atmospheric dynamics. Turbulent Shear Flows 4, 7–33.

Schertzer, D., Lovejoy, S., 1987a. Physically based rain and cloud modeling by anisotropic multiplicative turbulent cascades. J. Geophys. Res. 92, 9693–9714.

Schertzer, D., Lovejoy, S., 1989. Nonlinear variability in geophysics: multifractal analysis and simulation. In: Pietronero, L. (Ed.), Fractals: Physical Origin and Consequences. Plenum, New York, pp. 49–79.

Schertzer, D., Lovejoy, S., Lavallée, D., Schmitt, F., 1991. Universal hard multifractal turbulence: theory and observation. In: Sagdeev, R.Z., Frisch, U., Moiseev, A.S., Erokhin, A. (Eds.), Nonlinear Dynamics of Structures. World Scientific, Singapore, pp. 213–235.

Schertzer, D., Lovejoy, S., 1992. Multifractals in geophysics, course notes. AGU–CGU–MSA Spring Meeting, May 11, 1992.

Schertzer, D., Lovejoy, S., Schmitt, F., 1995. Structures in turbulence and multifractal universality. In: Meneguzzi, M., Pouquet, A., Sulem, P.L. (Eds.), Small-scale Structures in 3D Fluid and MHD turbulence, Springer-Verlag, Berlin. Lect. Notes Phys. 462, 137–144.

Schertzer, D., Lovejoy, S., 1997. Universal multifractals do exist! Comments on ''A statistical analysis of mesoscale rainfall as a random cascade'' by Gupta, V.G., Waymire, E.C. J. Appl. Meteor., in press.

Schertzer, D., Lovejoy, S., Schmitt, F., Chigirinskaya, Y., Marsan, D., 1997. Multifractal cascade dynamics and turbulent intermittency. Fractals, in press.

Seuront, L., Schmitt, F., Schertzer, D., Lagadeuc, Y., Lovejoy, S., 1996a. Multifractal intermittency of Eulerian and Lagrangian turbulence of ocean temperature and plankton fields. Nonlinear Proc. Geophys. 3, 236–246.

She, Z.S., Leveque, E., 1994. Universal scaling laws in fully developed turbulence. Phys. Rev. Lett. 72, 336–339.

She, Z.S., Waymire, E., 1995. Quantized energy cascade and log-poisson statistics in fully developed turbulence. Phys. Rev. Lett. 74, 262–265.

Silas, P., Lovejoy, S., Schertzer, D., 1993. Single phase diffusion in multifractal porous rock. 12–15/10/1993 Proc. Hydrofractals 93, Ischia, Italy, pp. C1–6.

Silas, P., 1994. Diffusion in one dimensional multifractal. M.Sc. Thesis, Mc Gill University, Montreal.

Steele, J.H., 1985. A comparison of terrestrial and marine ecological systems. Nature 313, 355–358.

Weissman, H., Havlin, S., 1988. Dynamics in multiplicative processes. Phys. Rev. B 37 (10), 5994–5996.

Yaglom, A.M., 1966. The influence of fluctuations in energy dissipation on the shape of turbulent characteristics in the inertial interval. Sov. Phys. Dokl. 2, 26.

Zwanzig, R., 1982. Non-Markovian diffusion in a one-dimensional disordered lattice. J. Stat. Phys. 28 (1), 127–133.